NUMI-NOTE-BEAM-845

Radiation Dose Estimates for the Monitoring System

Debbie Harris, Nancy Grossman

Abstract

This document describes the expected doses to be received by components in the NUMI beamline monitoring system. Most of the calculations are done using particle fluences from the GEANT-based monte carlo GNUMI, but for the hadron monitor in front of the absorber, a comparison with MARS predictions is also made. The GEANT and MARS calculations agree for all particle types to within 20-40%, except for the prediction for neutrons, where GEANT predicts significantly more neutrons. For design purposes the more challenging neutron fluxes (and hence doses) will be assumed.

1 Particle Composition at Monitor Locations

Predictions for the particle composition at the monitoring locations come from the Geant-based beamline simulation, GNUMI. The program was run with extremely low cutoff values so that particles of even very low energies would be followed. Figure 1 shows the energy distributions for the different species of particles that arrive at the downstream hadron monitor location, averaged over the entire $1m^2$ area. Note that 99% of the protons which arrive at the downstream hadron mointor are 120 GeV protons, which presumably did not interact in the target.

The particle fluxes at the downstream hadron monitor depend critically on the distance from the center of the beamline, as can be seen in figure 1. In the center the flux is dominated by the protons, while at the outer edges the fluxes are mostly electrons and positrons. The fluxes of both muons and neutrons at the muon monitors are significantly less peaked as a function of the distance from the beam center, and are not shown. This plot is made assuming the downstream hadron monitor is located 80cm upstream of the hadron absorber–later in this document we will show how the fluxes and ultimately the doses change for different locations.

2 Calculations of Radiation Damage

When calculating the dose that components receive due to radiation that will pass through them, there are two different standard techniques. The most common technique is to calculate the energy deposited per unit length of material (dE/dx) for a given particle, and then sum up all the particles.

For charged particles, the flux required to deposit 1 Gray (or 100 rads) in material is simply $6.24 \times 10^9/cm^2/(dE/dx)$ where dE/dx is given in units of g/cm^2 [1]. dE/dx for charged particles is loosely a function of material, but also a function of $\beta\gamma$ of the particle, as can be seen in figure 2.

For neutrons, dE/dx has a very different energy dependence, and depends much more critically on what the material is. While for charged particles the difference between liquid hydrogen and solid metals is about a factor of 2 or 3, for neutrons the difference between H

Figure 1: Logarithmic energy distribution of particles reaching the downstream hadron monitor location.

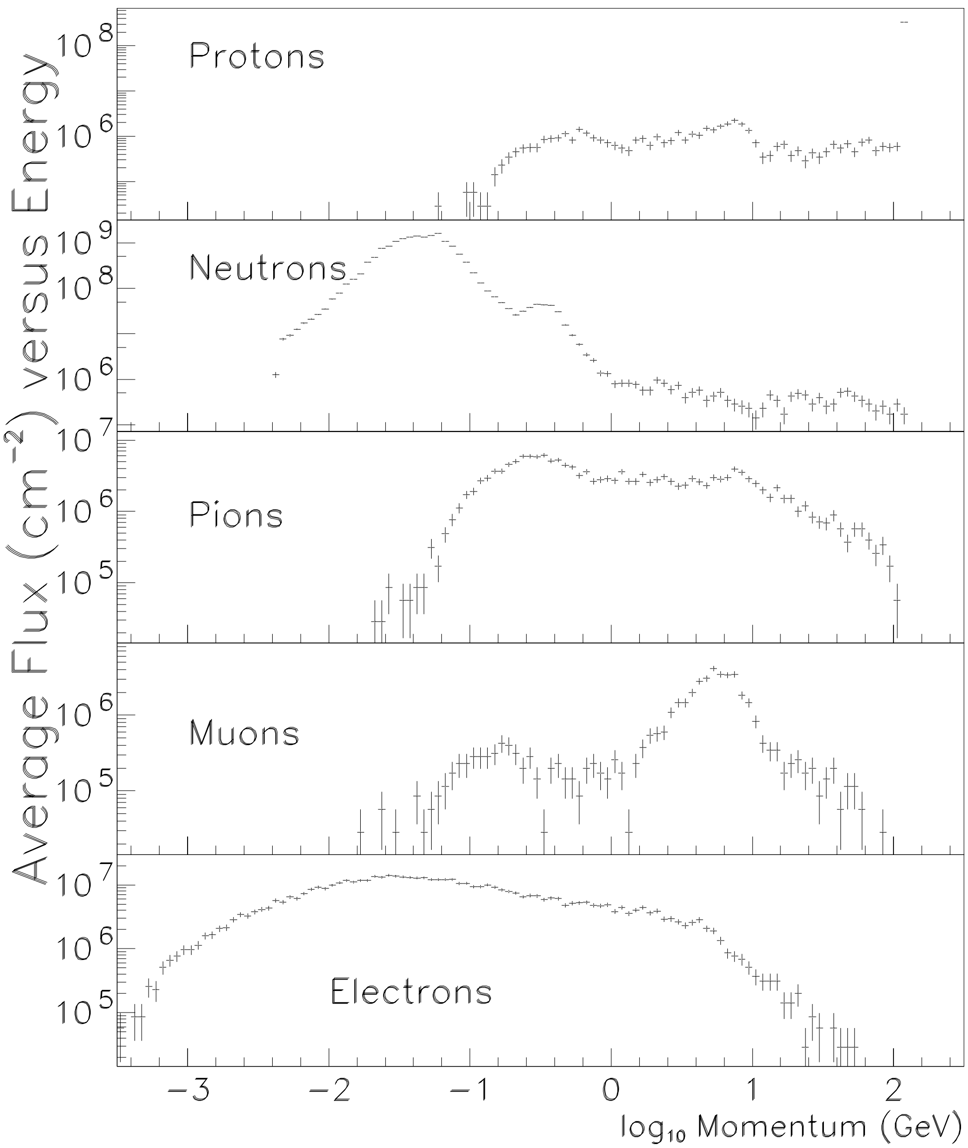

Figure 2: Fluxes and Doses at the downstream hadron monitor, as a function of particle type.

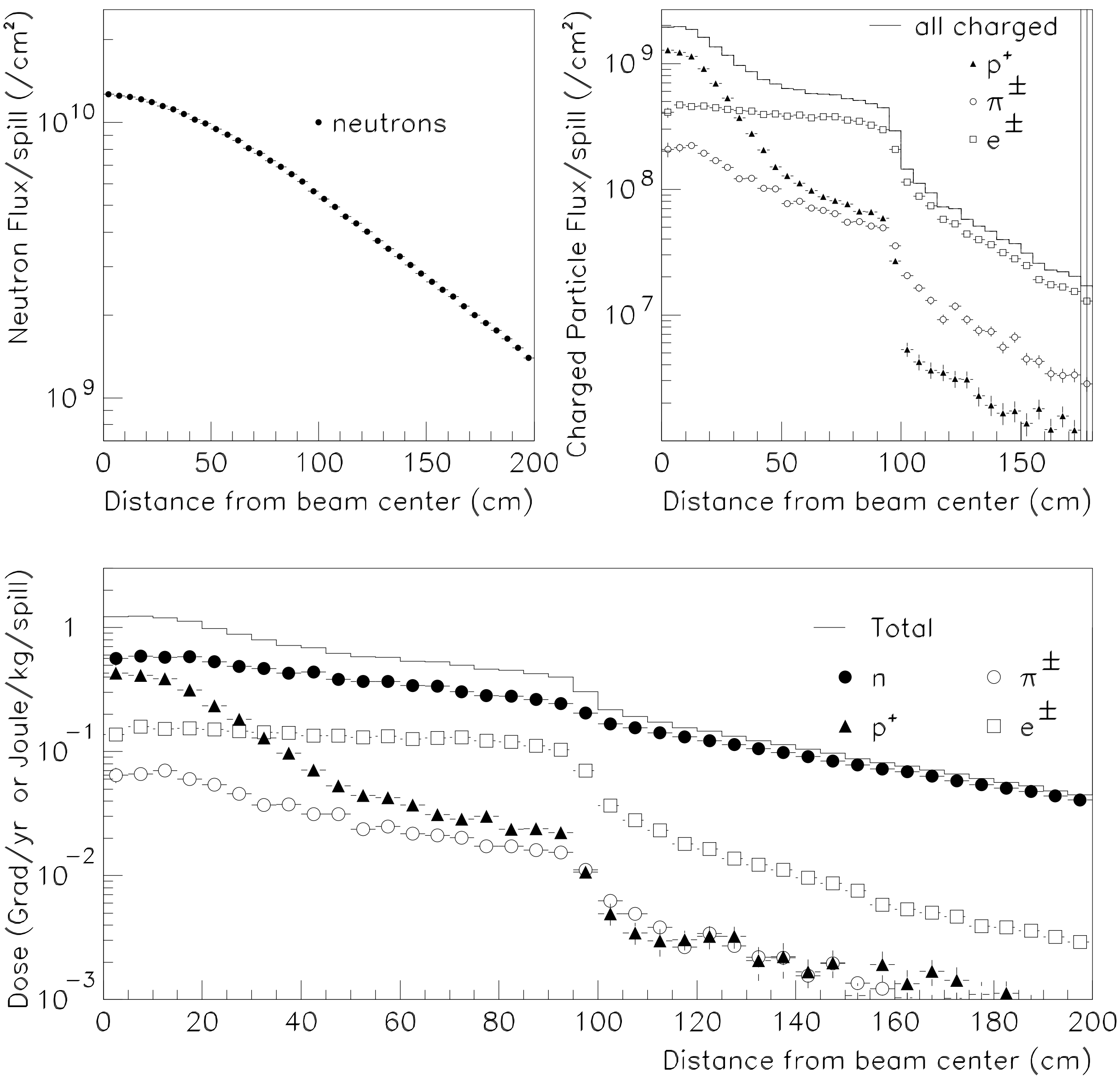

Figure 3: Energy loss rate in liquid (bubble chamber) hydrogen, gaseous helium, carbon, aluminum, iron, tin, and lead. Taken from reference [1].

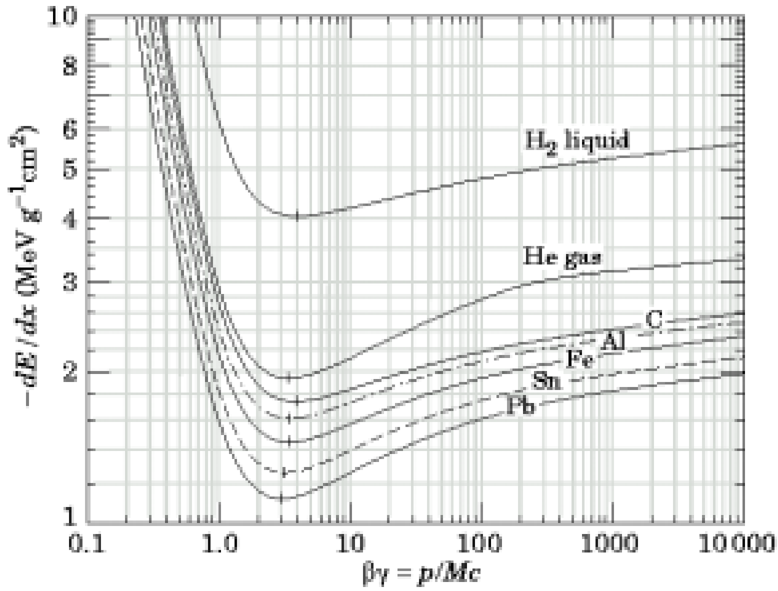

Figure 4: Neutron energy loss rate in various materials. Taken from reference [2].

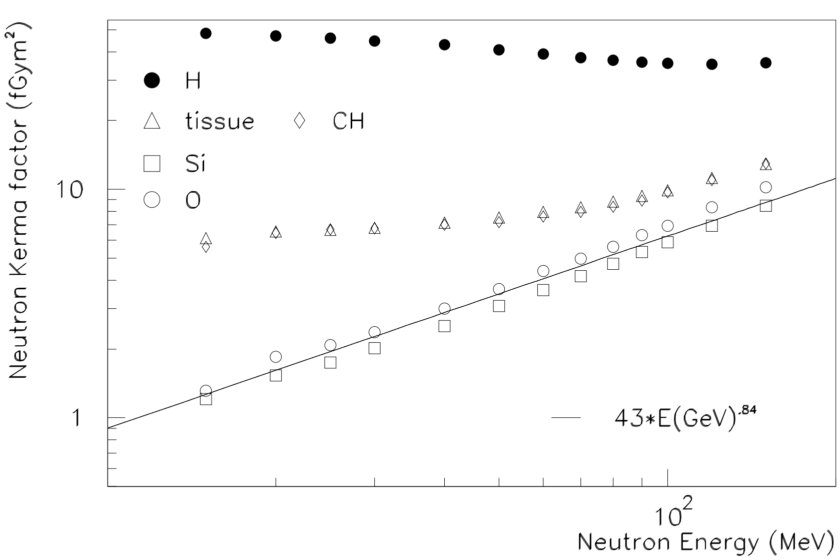

Figure 5: Dose to human tissue per unit flux for various charged particles, as a function of the charged particle energy. Taken from reference [3].

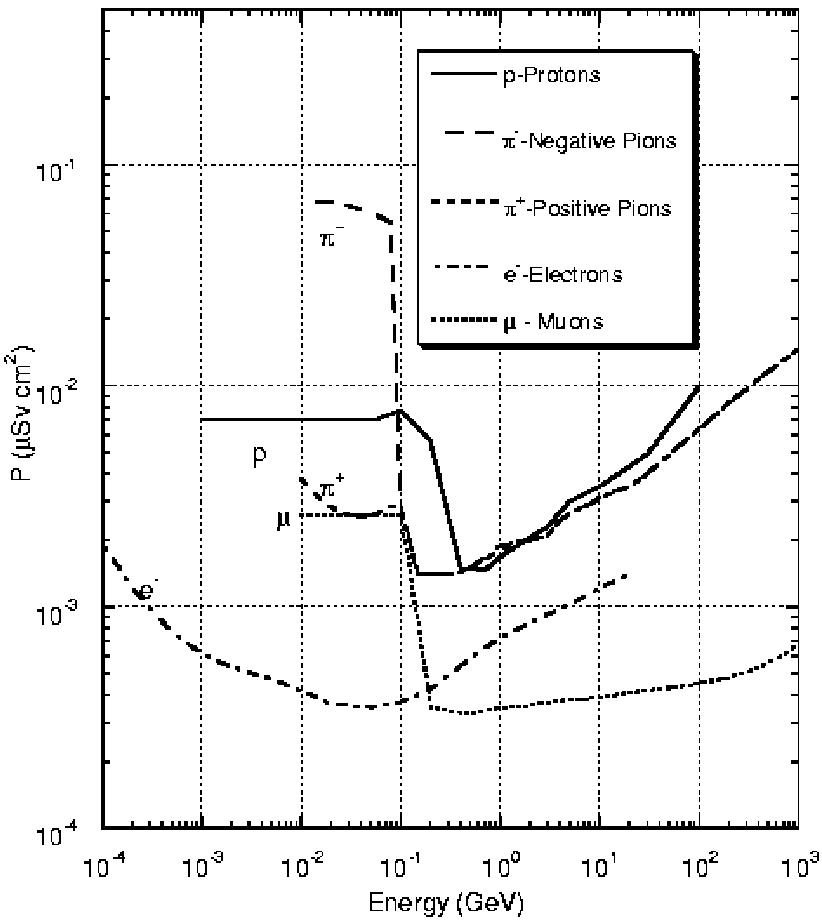

and other solids can be as much as a factor of 25. Figure 2 shows dE/dx for neutrons, as documented in reference [2].

A second technique used to calculate the doses, involves first converting the flux to a received dose in tissue (using the conversion factor which is in units of $Svcm^2$, shown in figure 2), and then converting from Sieverts to Gray using the quality factor, which for most particles is simply 1, but for neutrons of the relevant energies is a factor of 5. This technique would still produce the received dose in a material which has the chemical composition of human tissue, i.e. mostly C,H, and O. As can be seen in figure 2, there may be an additional factor of 2 or 3 in converting from a material that is pure Al, to a material that has significant hydrogen content.

3 Results

Table 3 gives the fluxes per spill of the various particles at the downstream hadron monitor, the conversion factor taken from [3], and the resulting doses from the two different calculations. The doses accumulated assume 4×10^{20} protons per year, and the fluxes assume that there are 4×10^{13} protons per spill. In the case of the dE/dx calculation, the energy distribution of the various particles is folded into the calculation, while the tissue calculation uses only an average conversion factor, although they do tend to depend logarithmically on

Figure 6: Left: Neutron Fluxes at the downstream hadron monitor, as a function of distance from the beam center, and also as a function of the distance between the monitor and the hadron absorber. Right: Total dose in Grad/year as a function of distance from the beam center, and as a function of the distance between the monitor and the hadron absorber.

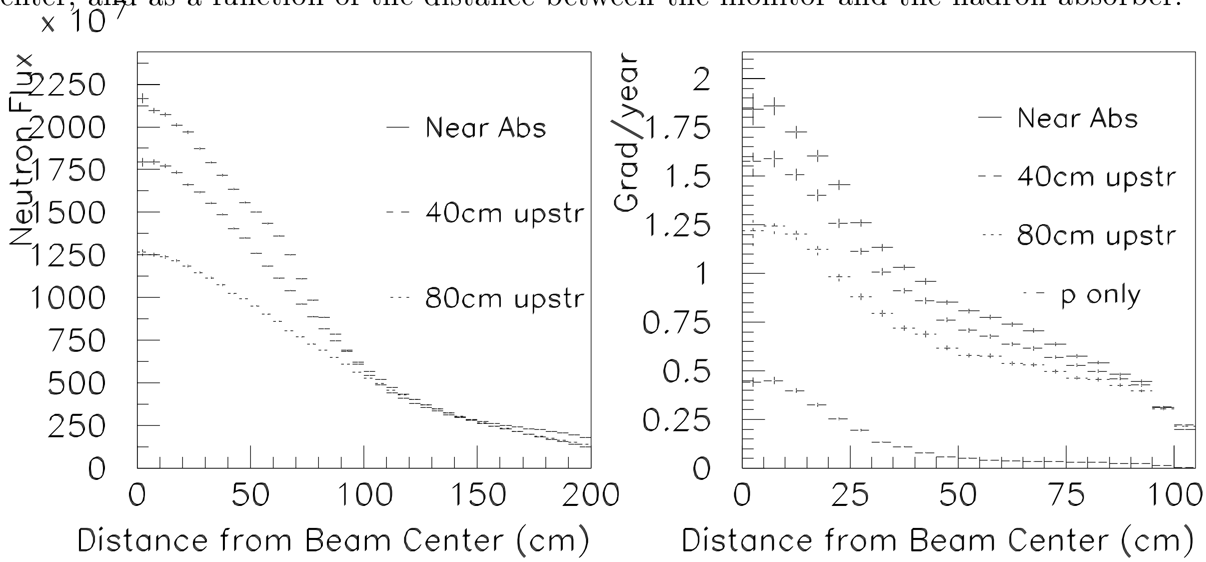

the energy of the particle. The fluxes and doses listed in the table are for a hadron monitor located about 80cm upstream of the hadron absorber. As is shown in figure 3 these fluxes rise as the hadron monitor is placed closer to the hadron absorber, the numbers in this table represent the optimal placement. In previous documents, the fluxes at a hadron monitor located 10cm upstream of the hadron absorber were given, which were significantly higher (as in figure 4 from the hadron specifications document).

Table 3 gives the fluxes and dose rates at the muon monitor locations. The simulation did not include delta rays, and as such the doses given are from muons and neutrons alone, since these are the only relevant particles which reach those monitor locations. The monte carlo statistical errors are shown since they are sizeable.

As can be seen by the table, the dose rates for the downstream hadron monitor change significantly as a function of distance from the beam center. Figure 1 shows the fluxes of neutrons and charged particles at the hadron monitor as a function of distance from beam center, as well as the dose as a function of distance. It is clear that at beam center the neutrons contribute about half of the total dose, while at distances past the decay pipe walls, over 99% of the dose is due to neutrons.

Although the downstream hadron monitor is primarily sensitive to the uninteracted protons from far upstream, the remainder of the particles arriving at the downstream hadron monitor are due to particles either created at the downstream vacuum window or splashing back from the hadron absorber. Figure 3 shows how the neutron flux at the center of the monitor can be reduced by moving the monitor usptream of the absorber by 80cm. There is only about 100cm between the vacuum window and the absorber front face, so this would be roughly the best one could do. Overall there is about a 40% reduction in neutron flux at 80cm upstream, and there are similar reductions in fluxes for electrons.

Table 1: Fluxes of various particle species that arrive at the downstream hadron monitor, and what dose they incur on the monitor, for two different calculations, as described in the text.

	Flux ($/cm^2/spill$)		Conversion Factor	dE/dx Dose Grad/year		Tissue Dose Grad/year	
Particle	$100 \times 100 cm^2$	Peak	($Sv \times cm^2$)	$10^4 cm^2$	Peak	$10^4 cm^2$	Peak
electrons	4.1E+08	4.1E+08	5E-10	0.14	0.14	0.21	0.21
pions	1.2E+08	2E+08	2E-09	0.038	0.063	0.24	0.41
muons	3.9E+07	3.7E+07	4E-10	0.013	0.013	0.016	0.015'
protons	3.7E+08	1.3E+09	1E-08	0.13	0.44	3.7	13
neutrons	1.1E+10	1.3E+10	5E-10	0.44	0.62	1.1	1.3
total				0.762	1.28	5.3	15

Table 2: Fluxes of muons and neutrons that arrive at the muon monitor locations, and what dose they incur on the monitor, for two different calculations, as described in the text.

Alcove	Particle	Flux ($10^7/cm^2/spill$)	Conversion ($Sv \times cm^2$)	dE/dx Dose (Mrad/year)	Tissue Dose (Mrad/year)
0	Muons	$1.1 \pm .07$	4E-10	3.5 ± 0.23	4.4 ± 0.3
0	Neutrons	9.3 ± 0.16	5E-10	1.8 ± 0.038	9.3 ± 0.16
0			Total	5.3 ± 0.2	13.7 ± 0.4
1	Muons	$0.28 \pm .04$	4E-10	0.88 ± 0.12	1.1 ± 0.16
1	Neutrons	0.12 ± 0.02	5E-10	0.018 ± 0.003	0.12 ± 0.019
1			Total	1.0 ± 0.1	1.2 ± 0.2
2	Muons	$0.12 \pm .03$	4E-10	0.4 ± 0.1	0.48 ± 0.1
2	Neutrons	0.0057 ± 0.004	5E-10	0.00044 ± 0.00031	0.0057 ± 0.004
2			Total	$.4 \pm 0.1$	0.5 ± 0.1

Table 3: Comparison of Fluxes and Dose Rates between MARS and GEANT, where a 20MeV cut has been put on all particles, and averaged over a 1m diameter disk, located 1m upstream of the absorber.

	n	$h^{\pm}$	γ	$e^{\pm}$	Muons	Dose/year
Job			$(/cm^2/spill)$			(rad)
MARS-AIR	2.8E+08	1E+09	6.1E+08	2.6E+08	3.4E+07	5.91026E+08
MARS-Fe/Al	3.6E+08	1.2E+09	7.7E+08	3.2E+08	3.9E+07	7.42949E+08
GEANT (air)	9.5e9	0.57e9	8.6e8	3.2e8	4.2e8	7.0e8

4 Comparison with MARS

One important thing to do is to compare with the fluxes and dose rates calculated by the MARS code, which has been benchmarked against many data sets. Although the calculations above assume dE/dx rates for ceramic, which are not very different from those for other materials, no showering was assumed in the hadron monitor itself. To compare the exact same quantities with MARS, a run was originally done with two 1m diameter disks of both aluminum and steel, comprising a "hadron monitor", and a separate run was made with the same two slabs, but filled with air. So the fluxes and dose rates in the "air" job should correspond to the those in GNUMI. Also, there was a minimum 20MeV cut on particles in MARS, so the same cut was made in GNUMI (for this table alone!) to compare to MARS. Table 4 gives the fluxes of different particle types, averaged over the 1m diameter disk, for the two mars jobs, and GNUMI. Note that for all the different particle types the two predictions are in agreement, except for the neutron flux. MARS predicts about a factor of 30 fewer neutrons than GEANT. The received dose in GNUMI is about half from charged particles, half from neutrons, so the two calculations for dose rates (not including the neutrons) are about a factor of two off, but ignoring the differences in particle production, the two dose rates in the two jobs are comparable, at slightly less than 1 Grad averaged over a 1m diameter disk. Figure 4 shows the regions defined in a MARS run that was done before the hadron monitor was included. To understand what the dose rates are in areas where cables for the hadron monitor will be, we list in table 4 the doses received in all of the various locations indicated in this figure.

Figure 7: Regions defined in the MARS program.

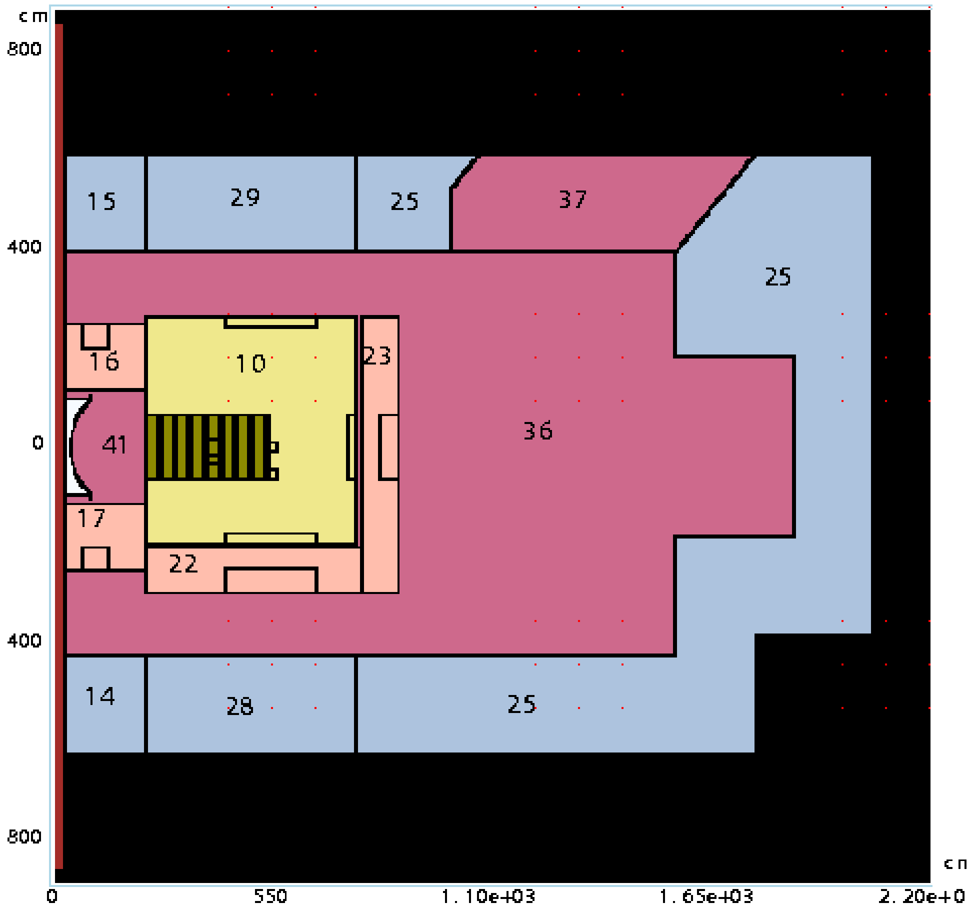

Table 4: Calculated Dose Rates from the MARS program with the geometry defined above.

Zone Number	Region	Dose Rate (/year)
	Decay Pipe Window	4.3 Grad
41	Air Upstream of Absorber	3.0 Grad
2	First 12" of Aluminum in Absorber	10.6 Grad
10	Steel Surrounding Aluminum Core	32.5 Mrad
16,17	Concrete surrounding decay pipe	15 Mrad
23	Concrete downstream of Steel	0.50 Mrad
36	Air outside Absorber Shielding	0.40 Mrad
22	Concrete east of Steel	40 krad
37	Entrance to Labyrinth	< 10 krad (3.4 ± 3)

Figure 8: Fluxes (top) and Particle compositions (bottom) at the downstream hadron monitor as a function of distance from the beam centerline. The information for the "target in" configuration is of course the one relevant for long term radiation doses.

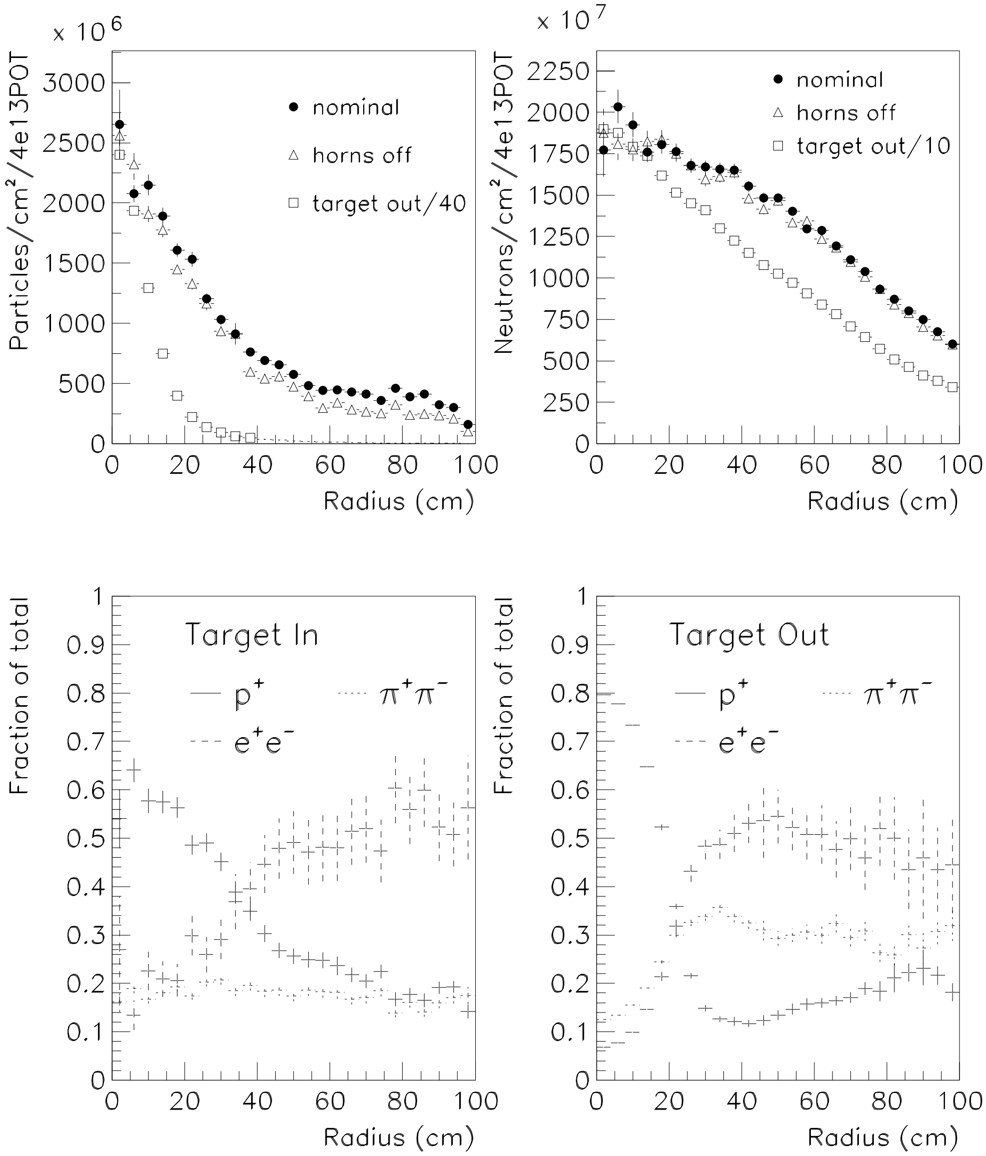

References

[1] Particle Data Group, 2000.

[2] D.V.Gorbatkov, V.P.Kryuchkov, O.V. Sumaneev, “Neutron Kerma Factors for tissue and particle detector materials from 15 to 150MeV”, Nucl. Instr. Meth. **A388** 260 (1997)

[3] J.D. Cossairt, “Radiation physics for personnel and environmental protection”, FERMILAB-TM-1834, (1993)